Effect of specimen size and shape on the mechanical properties measured on plugs subsampled from sidewall cores

Giorgio Volonté[1,*], *Jørn* Stenebraten[2], and *Euripides* Papamichos[2]

[1]Eni S.p.A., 20097 San Donato Milanese, Italy
[2]SINTEF Industry, NO-7465 Trondheim, Norway

Abstract. For several disciplines, the increasing acquisition of rotary sidewall cores (RSWC) in the oil and gas industry gives the opportunity for more extensive experimental rock characterization but, on the other hand, the limited amount of recovered material, their shape and orientation are not optimal for geomechanical experiments in the triaxial cell. These drawbacks can be overcome by performing experiments on properly shaped and oriented small diameter plugs subsampled from the RSWCs. These plugs are smaller than conventional ones, so the effects of both specimen shape (i.e., length over diameter L/D ratio) and size (i.e., diameter) on strength, stiffness (i.e., Young's modulus), and dilation (i.e., Poisson's ratio) must be carefully considered. In this work, an experimental study on specimen shape and size effects on rock mechanical properties has been tailored to materials and testing conditions generally encountered in petroleum related geomechanics. Triaxial compression experiments at three confining pressures have been performed on outcrop analogues of typical reservoir rock lithologies, i.e., two sandstones and two limestones, and within a range of shapes and sizes relevant for specimens prepared from RSWCs with emphasis on 10 mm diameter specimens. The strength, stiffness and dilation results were analysed and compared with relevant data and relations available in the literature. Then, analytical equations, useful for the practice of geomechanical experimental studies on RSWCs, have been derived to correlate mechanical properties measured on specimens of any shape or size to the ones obtainable on reference specimens.

1 Introduction

Several wellbore and field scale problems in the Oil & Gas industry require dedicated geomechanical experimental characterization that is usually performed on material acquired from 3” to 4” diameter bottom hole cores (BHCs). However, in the recent years, industry is increasingly promoting the partial replacement of bottom hole cores with 1”1/2 diameter rotary sidewall cores (RSWC) since the cost of their acquisition is lower. It should be noticed that RSWCs provide an opportunity to several disciplines to acquire data already from exploratory wells or from non-reservoir facies with a limited additional expense. But, on the other hand, geomechanical testing, e.g. triaxial compression tests, requires the use of multiple plugs sampled at the same depth interval and properly oriented with respect to bedding or in situ stresses. These requirements, easily satisfied by conventional plugs sampled on BHCs, requires that RSWCs are subsampled to plugs whose dimensions are smaller than conventional ones.

Since measured mechanical properties are affected by specimen shape (i.e., length over diameter L/D ratio) and size (i.e., diameter D), in this work an experimental study on their effect on the strength, stiffness (i.e., Young's modulus), and dilation (i.e., Poisson's ratio) of the rock has been tailored to materials and testing conditions generally encountered in petroleum related geomechanics. In the literature several experimental studies investigate these effects and especially the effects on the unconfined compressive strength (UCS) (e.g., [1] and references within). However, most of them are based on larger samples or on lithology not common in the Oil & Gas industry. A summary of these experimental evidence is presented in the following paragraphs.

1.1 Effect of specimen size and shape on strength

Generally, the compressive strength of the rock increases with decreasing L/D ratio especially for values lower than 2.5. The reasons for this increase may be related to the impediment of the development of an inclined shear band for failure in short specimens. For such specimens the inclination of the failure plane (shear band) is such that it meets the loading platens and thus it cannot develop freely, while in more slender specimens it meets the side of the specimen and can form a kinematically possible failure mechanism. Another reason is the confinement due to friction at the loading platens which is more dominant in shorter specimens and provides lateral support to the specimen. It should be anyway highlighted that, for small samples, these boundary conditions may dominate the failure, not the intrinsic failure mechanisms. Experimental data for granite specimens presented in [2] are an example of such behaviour. Figure 1 plots various correlations, based on experimental results, that have been proposed in the literature [1,3,4,5] to describe the shape effect on strength. The ASTM suggested equation for the correction of measured strength is also shown [6].

Regarding the size effect, a decrease in strength is observed with increasing specimen size since, statistically, with larger specimens there is a larger probability to include critical flaws in the sample that may lead to specimen failure. Moreover, the strength of a specimen increases as the ratio of specimen size to internal length of the rock, e.g. grain size, decreases. This behaviour has been highlighted by the experimental results reported in [7] and described, e.g., by the following equation proposed in [8]:

$$\frac{UCS}{UCS_{D_{ref}}} = \left(\frac{D_{ref}}{D}\right)^{k} \quad (1)$$

* Corresponding author: giorgio.volonte@eni.com

where D_{ref} is the diameter of the reference specimen and k a parameter equal to 0.18 for D_{ref} equal to 50 mm.
However, in [9] it is suggested that the relation presented in [8] is rather valid for hard rocks whereas for carbonates and sandstones a peak strength is observed between 38-54 mm diameter specimens as shown in Figure 2 where the strength decreases in either side of the peak.

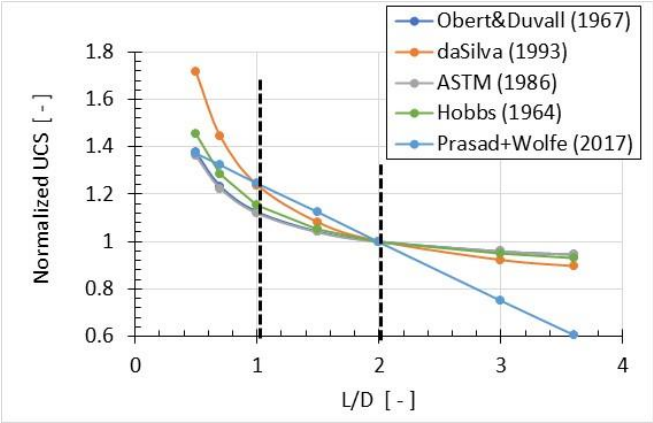

Fig. 1. UCS relations with L/D proposed by various investigators. The UCS is normalized with the UCS for L/D = 2. The dotted lines indicate the range of L/D ratios investigated in this study.

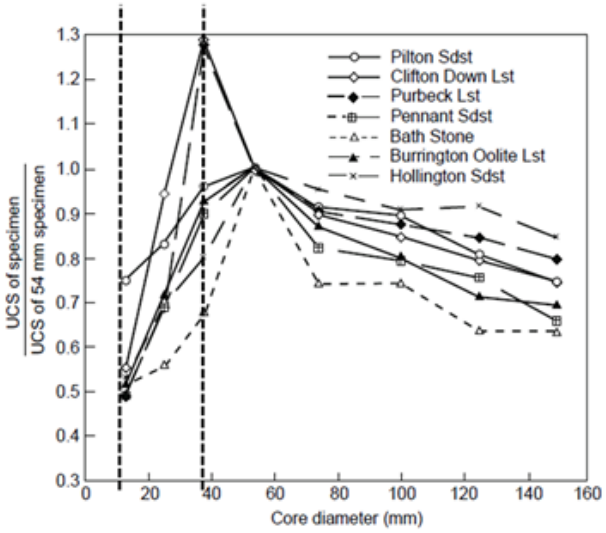

Fig. 2. UCS of seven sedimentary rocks measured on samples of eight different diameter [9]. Values are normalized with respect to the strength of the 54 mm diameter sample of the corresponding rock type. The dotted lines indicate the range of diameters investigated in this study.

1.2 Effect of specimen size and shape on stiffness

Although the effect of shape and size on stiffness has not been studied as extensively as that on strength, most of the data in the literature indicate that it is relatively small or that there is a significant scatter in the observations. In [10] it is shown that the stiffness modulus is practically independent of the shape. However, both an increase and a decrease of stiffness with increasing L/D ratio have been reported in [11] for kersantite rock and in [12] for Berea sandstone, respectively. In [13] a small, if any, increase in stiffness with increasing L/D in a granite is highlighted. Reference [14] also reports an increase in stiffness with increasing L/D ratio in Red Wildmoor sandstone, but this increase was attributed to the bedding error in the contact between the specimen and the loading platens.
Similarly, the size does not seem to have a large effect on the stiffness of the rock. In [7] and [13] a small effect of the size of granite specimens on stiffness is reported. Reference [13] presents a small increase in stiffness, while [15] reports a larger increase with increasing diameter in limestones. All the experimental results presented are for diameters in the range of 45 – 900 mm, which are larger than the diameters analysed in this study which were in the range of 10-38 mm.

1.3 Effect of specimen size and shape on dilation

The effect of shape and size on dilation, i.e. on the tangent Poisson's ratio ν_{50}, has been studied even less than that on stiffness. In [10], from the few available data, a decrease of Poisson's ratio with increasing L/D ratio for granitic rocks is reported. Reference [12] shows a decrease, no effect or increase of Poisson's ratio with increasing L/D for Berea sandstone with no clear effect of the confining stress. In [13] a small, if any, effect on Poisson's ratio is shown for a granite. Similarly, the size does not seem to have a consistent effect on the Poisson's ratio. In [13] variable effects of the size of granite specimens on Poisson's ratio is seen.

2 Experimental program

The effect of the specimen shape and size on the triaxial compressive strength (TCS), tangent Young's modulus E_{50} and tangent Poison's ratio ν_{50} at 50% the peak deviatoric stress was studied experimentally through conventional triaxial compression (CTC) tests at 0.5, 10 and 30 MPa confining stresses. Tests on two sandstones, Carbon Tan (CT) and Saltwash North (SWN), and two limestones, Indiana (IND) and Burlington (BURL), were performed. Table 1 lists the shape and size combinations that were studied experimentally by listing the typical number of tests that were performed. The repetition of tests performed with L/D = 2 specimens allowed to verify the repeatability of the experiments. Some dispersion of the results has been anyway observed (as shown in terms of standard deviation in the plots of the subsequent sections), especially for SWN and IND due to their more accentuated heterogeneity, but this scatter does not hide the observable trends when present. In the cases where tests were repeated also for different L/D ratios, similar repeatability was confirmed.

Table 1. Test matrix for the shape (L/D) and size (D) effect on the triaxial compressive strength, the tangent stiffness modulus E_{50}, and the tangent Poison's ratio ν_{50}. The table lists the typical number of tests performed for each lithology.

	***D* [mm]**		
L/D	**10**	**25**	**38**
1	1	-	-
1.5	1	-	-
2	3	3	3

Experiments were performed on oven dried specimens (60°C for 2 days). Samples were cored with a rotary core barrel and the end-surfaces were flattened with a surface grinder. The samples were mounted between steel end-pistons and surrounded with a Fluorinated Ethylene Propylene (FEP) heat shrink sleeve. A thin Teflon sheet was placed on each sample-end to reduce end-friction between the sample and end-pistons. Axial deformation was measured with three Linear Variable Differential Transformers (LVDTs), oriented in one plane, 120° apart. Radial deformation was measured with two pairs of strain-gaged cantilevers oriented orthogonally to each other and measuring the diametrical deformation at mid-height of the sample.

The testing was performed in a hydraulic servo-controlled load frame with digital feedback control and data acquisition. Confining pressure was ramped at 36 MPa/h and an axial strain rate of 1E-05 s^{-1} was used for the shearing segment.

The shape effect was studied on 10 mm diameter specimens with L/D equal to 1, 1.5 and 2, while the size effect was studied on specimens with L/D equal to 2 and diameters 10, 25 and 38 mm (Figure 3).

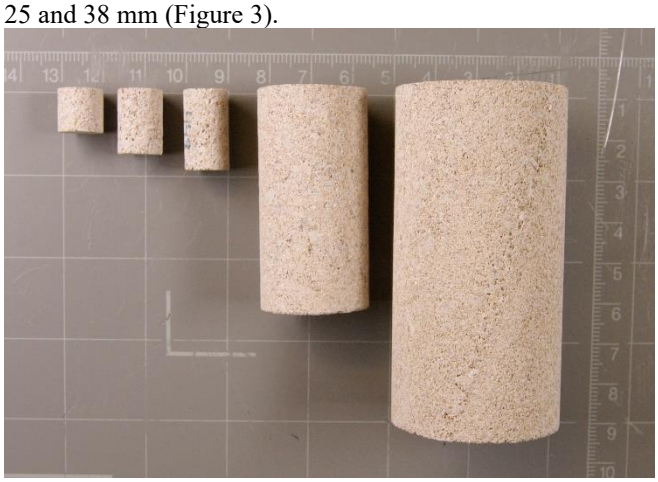

Fig. 3. Photographs showing the size range of tested samples.

3 Data analysis

The results of the experimental campaign were analysed to derive useful expressions for practical applications that correlate the mechanical properties measured on small specimen retrieved from RSWCs with those that would have been obtained through conventional plugs. For this purpose, a series of elaborations have been performed to reduce, as much as possible, the effect of specimen variability and, subsequently, to highlight or rule out eventual lithology dependent behaviours.

A measure of inherent sample variability can be the oven-dry bulk density of the specimens, since samples with higher density are expected to have a higher strength and stiffness. Indeed, some rocks in the present study showed a systematic difference in mechanical properties for a specific shape and size, that were prepared from blocks of rock with lower or higher density than the remaining samples. This resulted in an apparent lower or higher strength/stiffness, respectively. This effect is especially evident in the Carbon Tan samples whose data showed that the D = 25 mm specimens had systematically lower density and, thus, lower strength and stiffness (Figure 4a).

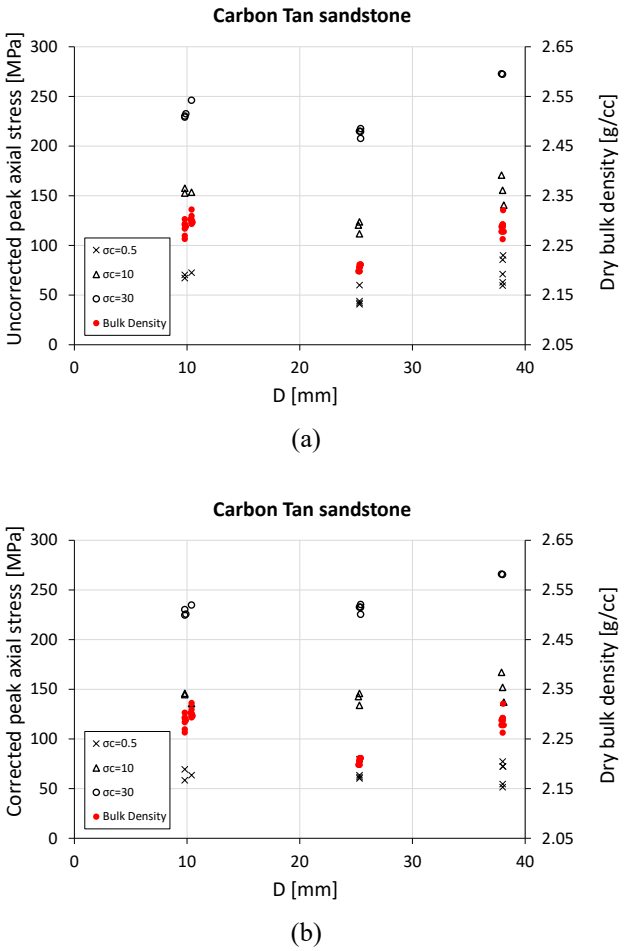

Fig. 4. Carbon Tan sandstone. Oven dried density and TCS before (a) and after (b) density correction.

Since this specimen variability influences the size and shape effects, correction correlations were considered necessary for Carbon Tan, Saltwash North, and Indiana. They were derived through the procedure described in the Appendix. An example of the corrected results is reported in Figure 4b for the strength of Carbon Tan sandstone: corrected data are slightly less sparse while trends are more evident and independent of the specimen density. This procedure was not applied to Burlington limestone which showed similar densities between all the samples.

To allow the comparison and the integration of data referring to different lithologies, all the corrected strength, moduli and Poisson's ratio values measured in the experiments at given confining pressure were averaged and normalized with respect to the corresponding average values obtained by testing reference dimension specimens. The reference dimensions have been assumed equal to 10 mm diameter with L/D = 2 for the study of shape effect and 38 mm diameter with L/D = 2 for the analysis of size effect.

Finally, all normalized values of strength, moduli and Poisson's ratio at given confining pressure were averaged across all rocks and integrated to derive correlations with size and shape independent of lithology. The data from the three confining stresses were not combined because the confining stress may play a role in the scale effect as suggested in the literature.

The outcomes of these analyses are described in the following sections where the obtained correlations with size and shape are reported.

4 Triaxial compressive strength

4.1 Shape effect

The values of normalized compressive strength in Figure 5 show some variability within each lithology at the various confining stresses. In some cases, the strength is higher at lower L/D ratios but in most it is lower. No clear difference can be identified between the four rocks. The plot in Figure 6a indicates that the strength of specimens with L/D = 1.5 and 2 are, for all practical purposes, similar. On the other hand, the strength of the specimens with L/D = 1 seems to be between 5% and 24% lower than the one of specimens with L/D = 1.5 and 2. This finding does not agree with similar findings in the literature which suggest an increase of strength with decreasing L/D ratio. In the range of L/D between 1 to 2, the literature suggests an increase of the strength of specimens with L/D = 1 compared to the one of specimens with L/D = 2 by anything between 12% [6] to 25.5% [1]. This difference can be explained by the small size of the specimens with L/D = 1 used in this study compared to the much larger diameters used in the studies in the literature. In this study the diameter is equal to 10 mm, and thus the specimens are 0.79 cm^3 cylinders with dimensions 20 or 30 times their grain size. Due to their relatively small size any damage during specimen coring and polishing may have a considerable effect on the strength.

For the practical applications involving 10 mm diameter specimens, we can combine a formula from literature, e.g., the one suggested by ASTM [6], for L/D > 2 with an equation that accounts for the apparent strength decline due to plug damage for L/D < 2. The combined formula is valid only for 10 mm diameter specimens and may be written as:

$$\frac{TCS_{L/D\_10}}{TCS_{2\_10}} = \begin{cases} 1.007 - e^{-3\frac{L}{D}} & \text{for} \quad \frac{L}{D} \leq 2 \\ 0.88 + \frac{0.24}{\frac{L}{D}} & \text{for} \quad \frac{L}{D} \geq 2 \end{cases} \qquad (2)$$

This equation is plotted in Figure 6b together with test data. In this formula and in all the following ones, the first part of the lower index indicates the L/D ratio of the specimen while the second part its diameter in mm. For example, TCS_{2_10} refers to the TCS of a specimen with L/D = 2 and D = 10 mm. Since, in this study, the shape effect has not been tested in other diameters, any of the formulas in the literature can be used for other diameter values, such as e.g., the following ASTM formula [6]:

$$\frac{TCS_{L/D\_D}}{TCS_{2\_D}} = 0.88 + \frac{0.24}{\frac{L}{D}} \quad \text{for} \quad D \geq 25 \text{ mm} \qquad (3)$$

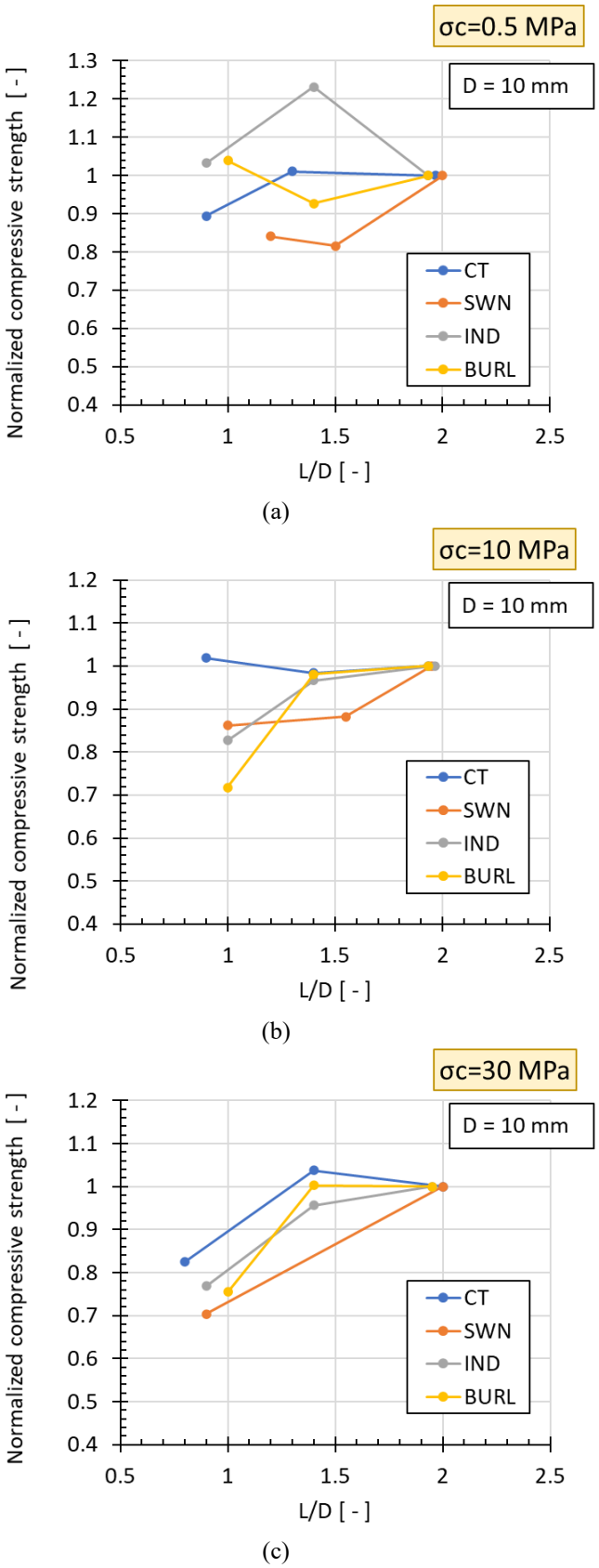

Fig. 5. Normalized TCS of all rocks vs. L/D ratio for confining stress σ_c = (a) 0.5, (b) 10 and (c) 30 MPa. All samples have diameter equal to 10 mm.

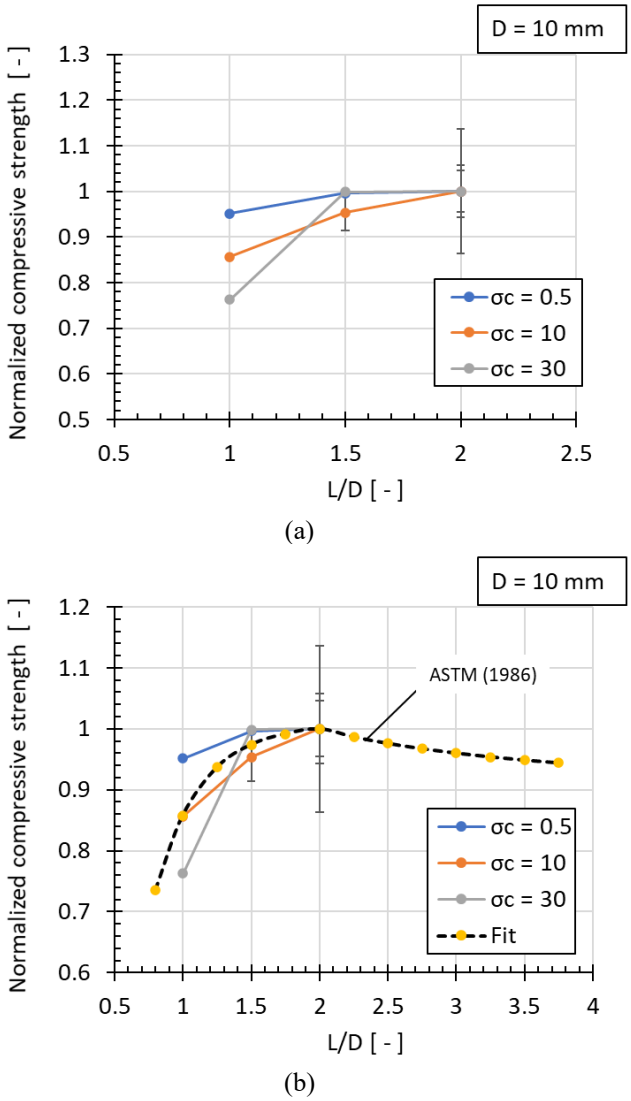

Fig. 6. Average normalized TCS of all rocks vs. L/D ratio for confining stress σ_c = 0.5, 10, and 30 MPa. All samples have diameter equal to 10 mm. In (a), data with standard deviation are reported while, in (b), they are superimposed with the Eq. (2) approximation.

4.2 Size effect

The values of normalized compressive strength in Figure 7 show some variability within each lithology at the various confining stresses. The variability is larger at low confining pressure σ_c = 0.5 MPa and lower for σ_c = 10 and 30 MPa. This reduction in variability with increasing confinement has been reported also in the literature, e.g., in [16] where earlier works are summarized saying that confining pressure tends to suppress the size effect on failure strength.

No clear difference is noticeable between the four rocks consistent for all confinement stresses. The plot in Figure 8a indicates that the strength decreases with decreasing size for all confining stresses, but the decrease is larger at low confinement, i.e. ca. 21% decrease, and smaller at higher confining stresses, i.e. ca. 7-10%. This decrease for small specimen diameters has also been reported in the literature [9,17] where it is suggested that the peak strength occurs for specimens with diameters between 38 and 54 mm. For larger sizes, the strength decreases again according to an exponential law [7,16,8]. The results in this study seem to corroborate the ones reported in [9] for limestones and sandstones (Figure 2).

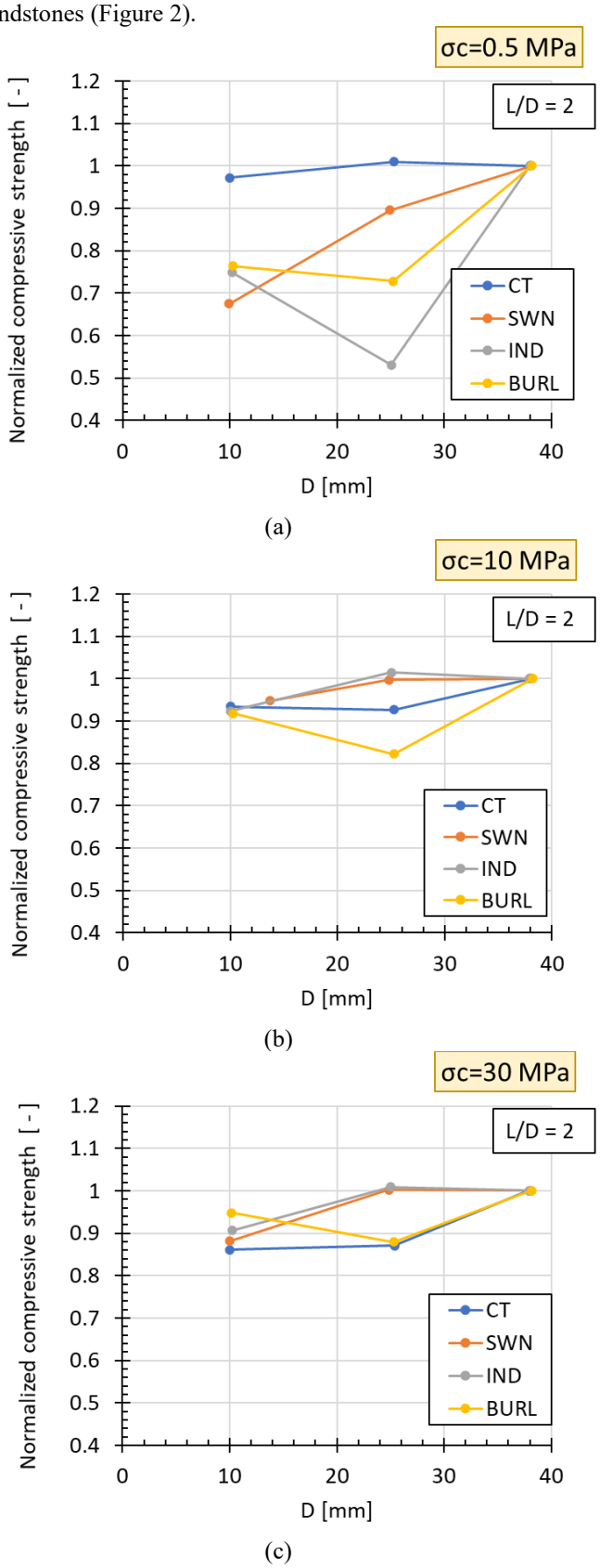

Fig. 7. Normalized TCS of all rocks vs. diameter for confining stress σ_c = (a) 0.5, (b) 10 and (c) 30 MPa. All samples have L/D ratio equal to 2.

It is thus proposed to combine the exponential decline formula reported in [8] for D > 38 mm with a linear formula where strength decreases with decreasing diameter. The linear relationship assumes a confining stress dependent slope to accommodate the effect of confining stress on the strength reduction. The combined formula may be written as:

$$\frac{TCS_{2\_D}}{TCS_{2\_38}} = \begin{cases} 1 - 0.13\left(1 + 2e^{-\frac{\sigma_c}{3}}\right)\left(1 - \frac{D}{38}\right) & \text{for } D \le 38 \\ \left(\frac{D}{38}\right)^{-0.18} & \text{for } D \ge 38 \end{cases} \quad (4)$$

where D is in mm. The approximation to the data using Eq. (4) is plotted in Figure 8b together with test data.

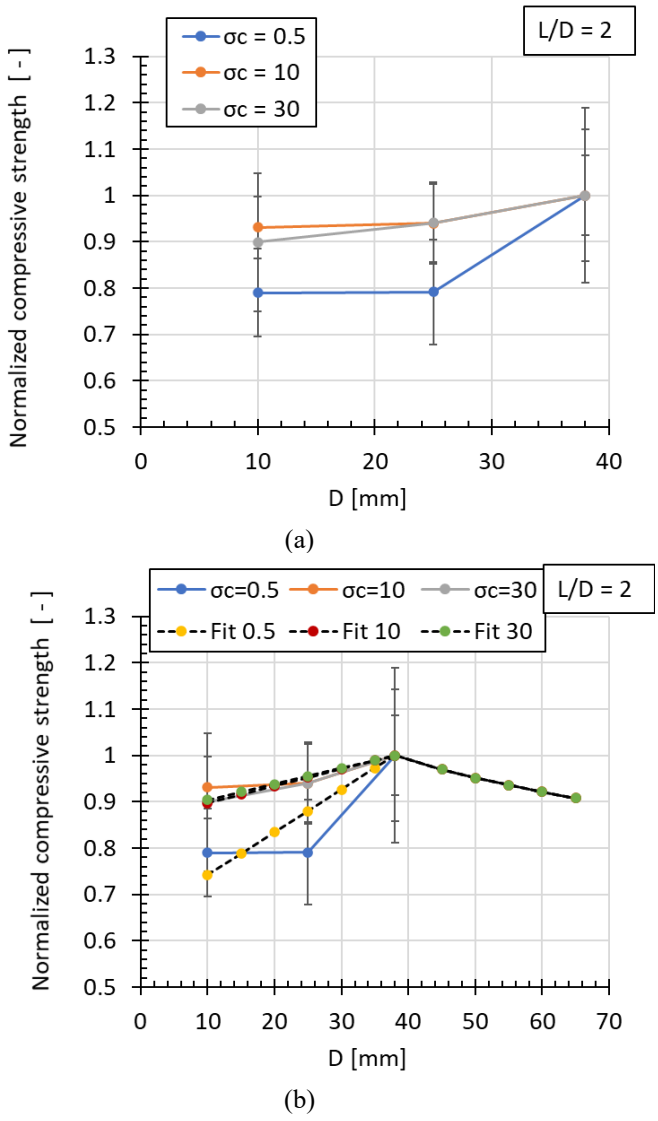

Fig. 8. Average normalized strength of all rocks vs. diameter for confining stress σ_c = 0.5, 10, and 30 MPa. All samples have L/D ratio equal to 2. In (a), data with standard deviation are reported while, in (b), they are superimposed with the Eq. (4) approximation.

4.3 Combined shape and size effect

Equations (2) or (3) and (4) can be combined to obtain the TCS value of a specimen with arbitrary shape L/D or size D:

$$\frac{TCS_{L/D\_D}}{TCS_{2\_38}} = \begin{cases} \left(0.88 + \frac{0.24}{L/D}\right)\left(\frac{D}{38}\right)^{-0.18} \; for \; D \ge 38 \\ \left(0.88 + \frac{0.24}{L/D}\right)\beta \; for \begin{cases} 20 \le D < 38 \\ or \\ D \le 20, L/D > 2 \end{cases} \\ \left(1.007 - 3e^{-3L/D}\right)\beta \; for \; D \le 20, \frac{L}{D} \le 2 \end{cases} \quad (5a)$$

where

$$\beta = \left[1 - 0.13\left(1 + 2e^{-\sigma_c/3}\right)\left(1 - \frac{D}{38}\right)\right] \quad (5b)$$

D is in mm and σ_c is in megapascals. It should be noted that Eq. (5) is based on both data derived in this study and data available in the literature. In particular, the relations for D >= 38 mm and for L/D > 2 are based on data and expressions from literature.

5 Tangent stiffness modulus

5.1 Shape effect

The values of the normalized stiffness moduli in Figure 9 show some variability within each lithology at the various confining stresses. In some cases, the stiffness is higher at lower L/D ratios but in most it is lower. No clear difference is noticeable between the four rocks. The plot in Figure 10 suggests that the stiffness modulus increases with increasing L/D. The modulus of the L/D = 1 specimens is between 27% and 58% lower than the L/D = 2 specimens. This difference can be observed also by comparing the stress-strain curves reported in Figure 11 for Saltwash North sandstone. This finding agrees with some results in the literature [11] although other results suggest a stiffness modulus independent of L/D [10], or decreasing with increasing L/D [12], or even both decreasing and increasing with L/D [15]. One of the reasons for the increase of stiffness with increasing L/D ratio is the bedding error associated with the specimen-piston interfaces when the axial strain is calculated from the deformation of the whole specimen [14]. Similarly to what observed for strength, another reason for the lower stiffness modulus of the low L/D ratio specimens is the small size of the specimens with L/D = 1, that allows any damage to have a considerable effect in stiffness as well as in strength.
For practical applications involving 10 mm diameter specimens, experimental data can be regressed with a linear function to model the shape dependency of stiffness modulus as:

$$\frac{E_{50\_L/D\_10}}{E_{50\_2\_10}} = 0.5 + 0.25\frac{L}{D} \quad (6)$$

which is also superimposed to test data in Figure 10. It should be highlighted that in this case data are quite sparse, especially for L/D=1.5. The shape effect has not been tested

in other diameters in this study and no formula is available in the literature.

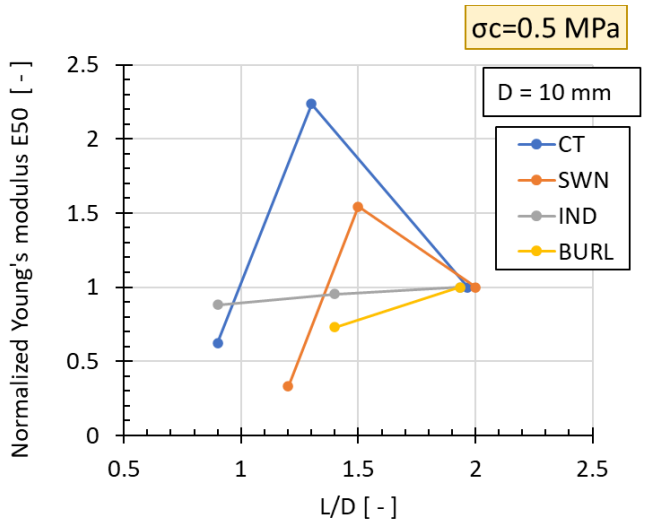

(a)

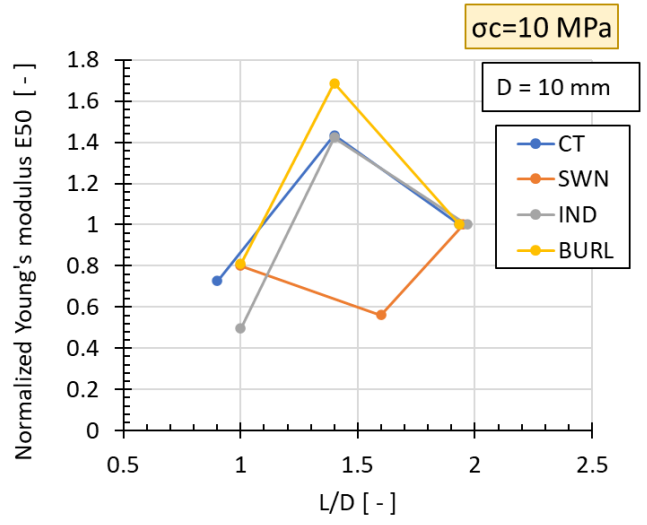

(b)

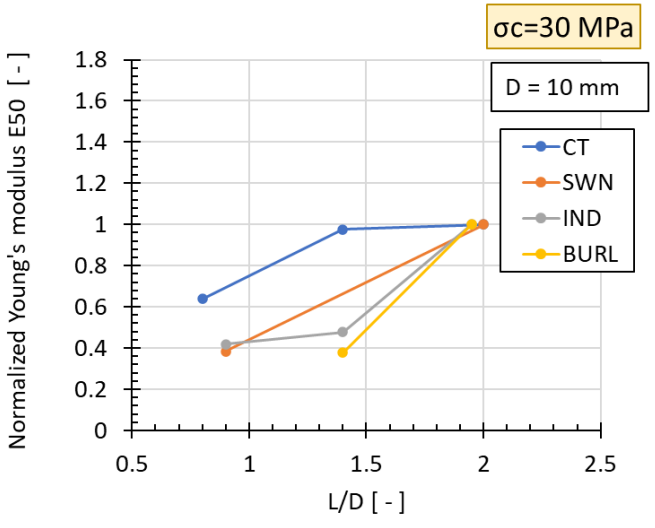

(c)

Fig. 9. Normalized E_{50} of all rocks vs. L/D ratio for confining stress σ_c = (a) 0.5, (b) 10 and (c) 30 MPa. All samples have diameter equal to 10 mm.

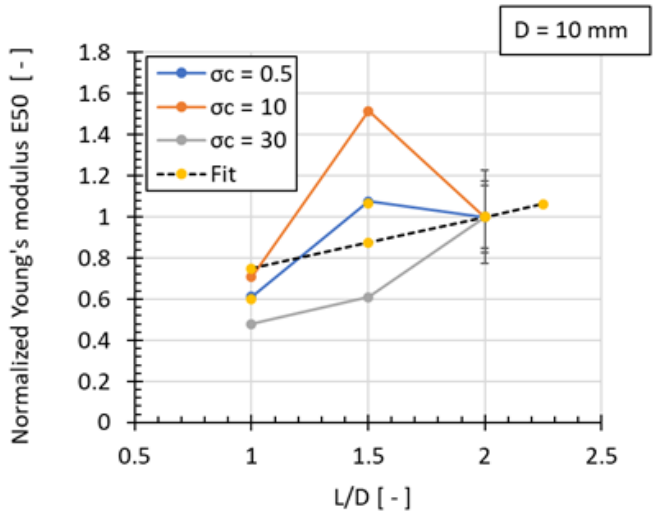

Fig. 10. Average normalized E_{50} of all rocks vs. L/D ratio for confining stress σ_c = 0.5, 10, and 30 MPa. All samples have diameter D = 10 mm. Standard deviation and approximation of the data with Eq. (6) are also reported.

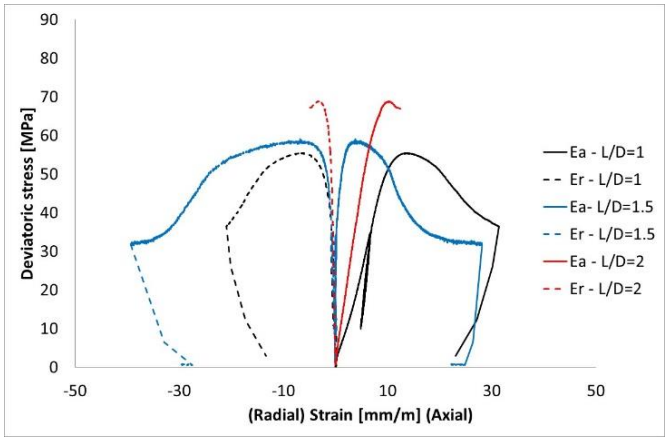

Fig. 11. Example of stress-strain curves for three experiments on Saltwash North sandstone at a confining pressure equal to 10 MPa.

5.2 Size effect

The values of normalized stiffness moduli in Figure 12 show some variability within each lithology at the various confining stresses. No clear difference is noticeable between the four rocks consistent for all confinement stresses (Figure 13). The plot does not demonstrate a clear dependency of the stiffness modulus with the size of specimen. Similar results have also been presented in [2] and [11]. However, in [15] an increase in stiffness with increasing size is shown. This behaviour can be observed also in Fig 14 where an example of stress-strain curves obtained by testing specimens of different sizes is reported for Saltwash North sandstone. According to the data, it is thus proposed to keep the stiffness modulus independent of the size of the specimen.

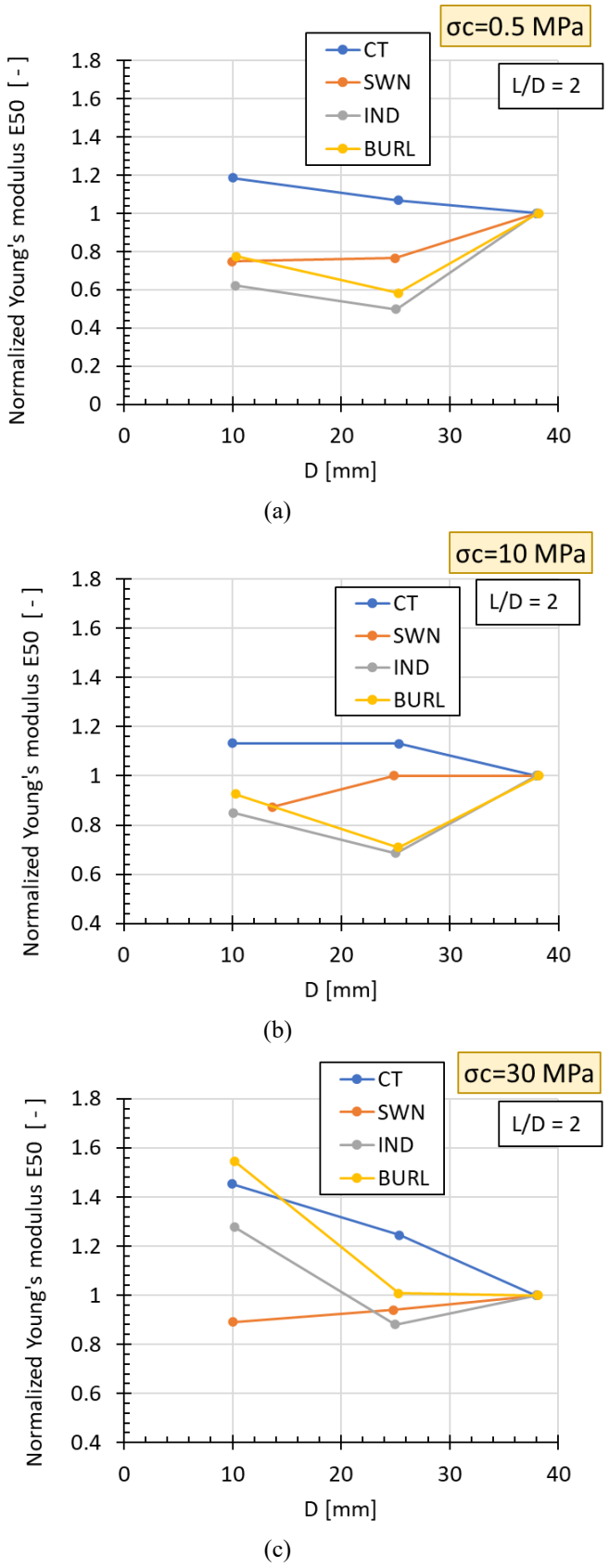

Fig. 12. Normalized E_{50} of all rocks vs. diameter for confining stress σ_c = (a) 0.5, (b) 10 and (c) 30 MPa. All samples have L/D ratio equal to 2.

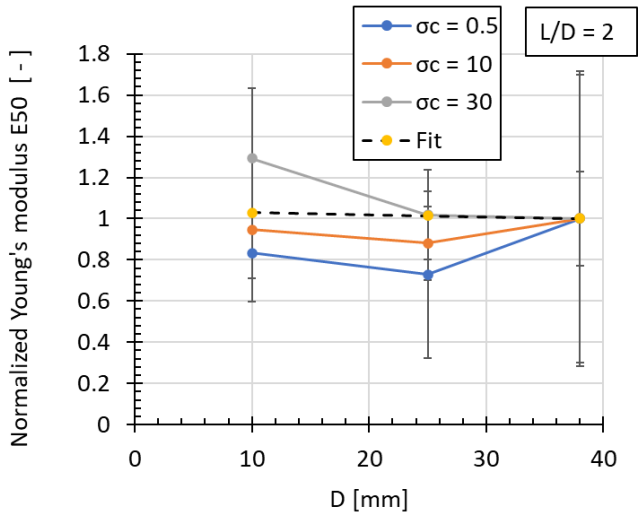

Fig. 13. Average normalized E_{50} of all rocks vs. diameter for confining stress σ_c = 0.5, 10, and 30 MPa. All samples have L/D ratio equal to 2. Standard deviations are also reported.

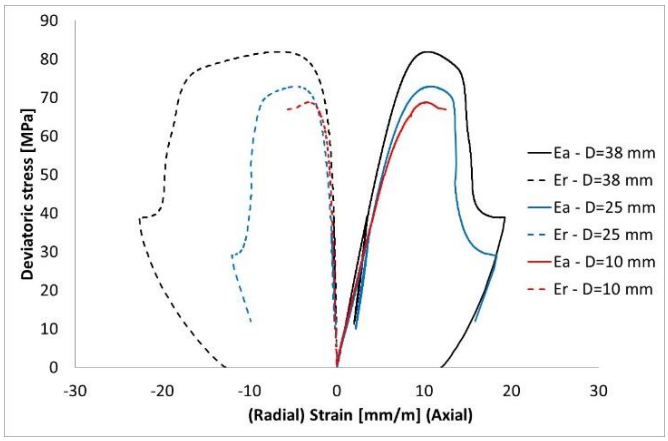

Fig. 14. Example of stress-strain curves for Saltwah North sandstone at 10 MPa.

5.3 Combined shape and size effect

In this study, the stiffness modulus appears independent of the specimen size. Therefore, only the shape effect formula Eq. (6) is necessary to obtain the E_{50} value of a specimen with arbitrary shape or size.

6 Tangent Poisson's ratio

6.1 Shape effect

The values of normalized Poisson's ratio in Figure 15 show some irregular variability within each lithology at the various confining stresses. In some cases, the dilation is higher at lower L/D ratios but in other cases it is lower.

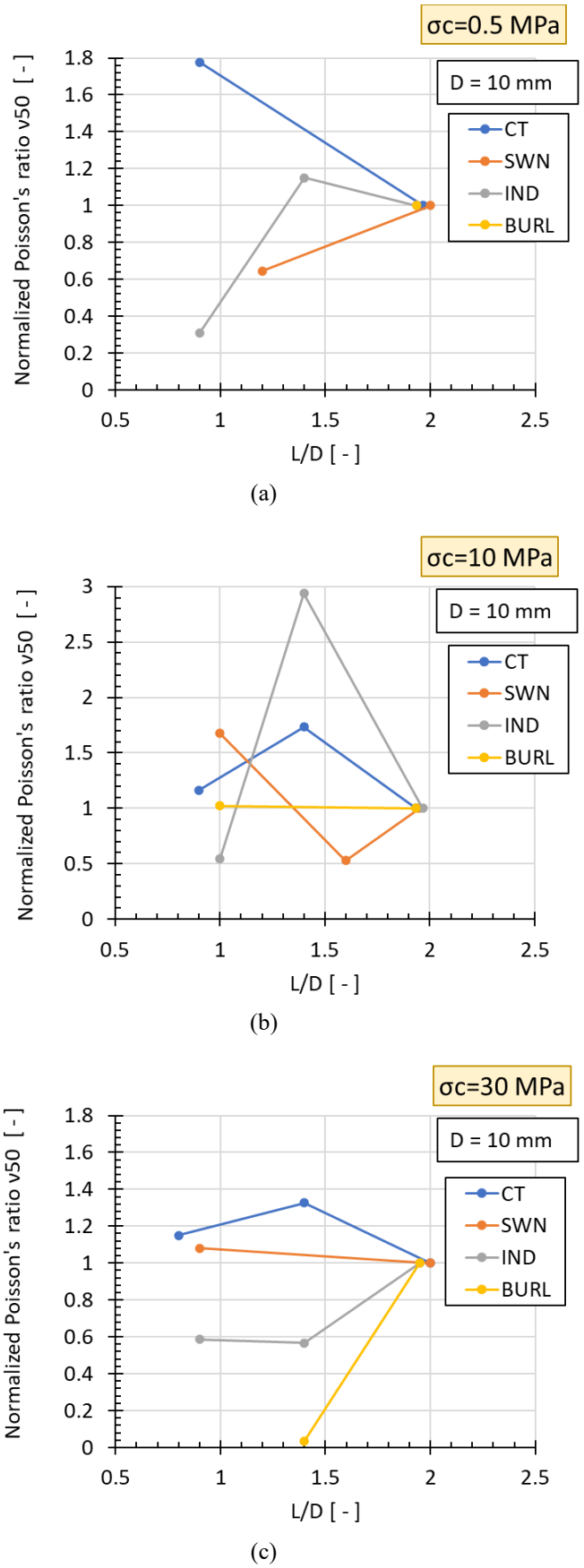

Fig. 15. Normalized v_{50} of all rocks vs. L/D ratio for confining stress σ_c = (a) 0.5, (b) 10 and (c) 30 MPa. All samples have diameter equal to 10 mm.

An increase of dilation with increasing L/D ratio may be expected due to the frictional effect in the interfaces between the platens and the specimen which may act as confinement and restrain lateral deformation. For shorter specimens, this effect may be more pronounced because the mid-height of the specimen, where the lateral deformation is measured, is closer to the loading platens. Despite that, experimental data show that Poisson's ratio increases modestly, if any at all, with increasing L/D (Figure 16). So, no correction of dilation measurement as function of L/D ratio is considered needed. It should be anyway highlighted that, as for Young's modulus, results are quite scattered for L/D = 1.5.
The shape effect has not been tested in other diameters in this study and no correlation in the literature is available.

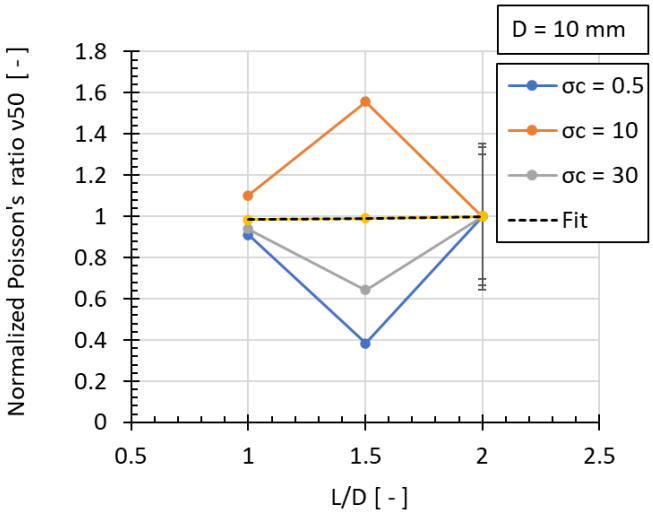

Fig. 16. Average normalized v50 of all rocks vs. L/D ratio for confining stress σ_c = 0.5, 10, and 30 MPa. All samples have diameter equal to 10 mm Standard deviation is also reported.

6.2 Size effect

The values of normalized Poisson's ratios in Figure 17 show little variability within each lithology at the various confining stresses, more accentuated at a confining pressure of 30 MPa especially for Indiana and Burlington limestones. Indeed, in these cases, the plot shows a decrease of the Poisson's ratio with increasing diameter which however is mostly influenced by the scatter of experimental results. At other confining stresses, no size effect is observed.
The overall trend of experimental data can be regressed with a linear function (Figure 18) to model the size dependency of Poisson's ratio as:

$$\frac{v_{50\_L/D\_10}}{v_{50\_2\_38}} = 1.2 - 0.0054D \qquad (7)$$

where D is in mm.

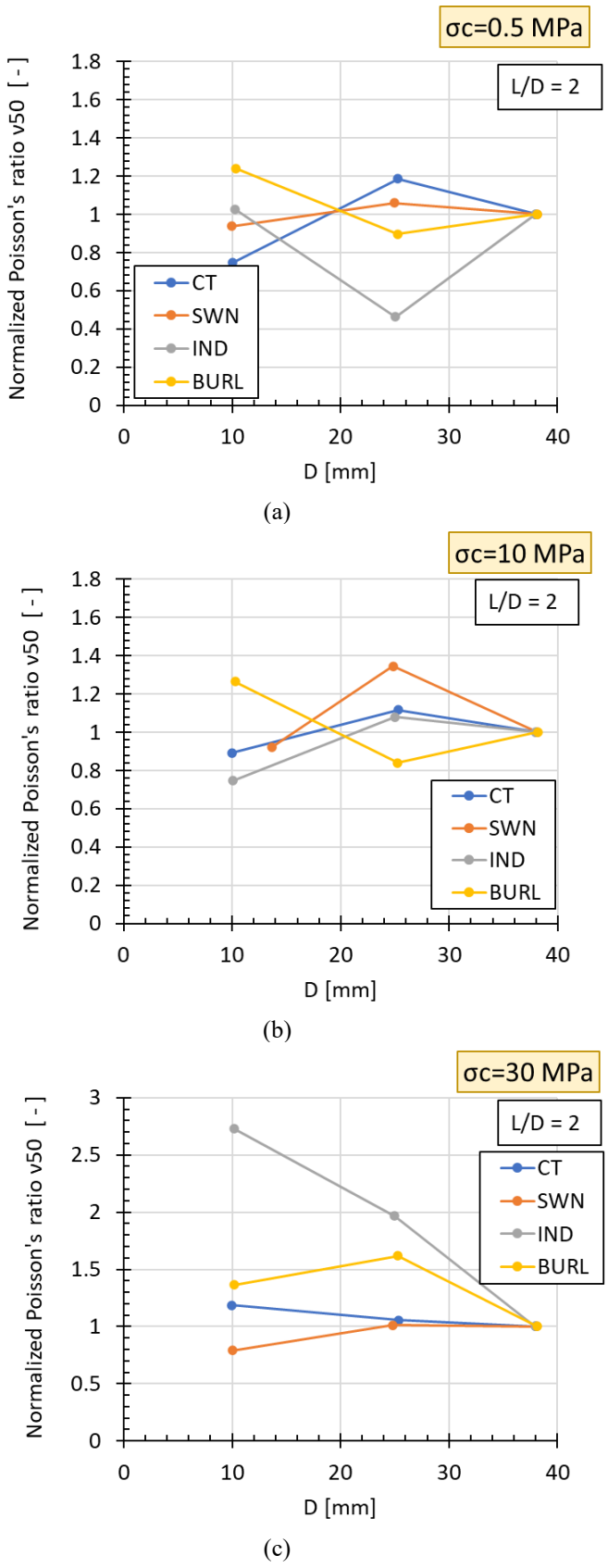

Fig. 17. Normalized ν_{50} of all rocks vs. Diameter (D) for confining stress σ_c = (a) 0.5, (b) 10 and (c) 30 MPa. All samples have L/D ratio equal to 2.

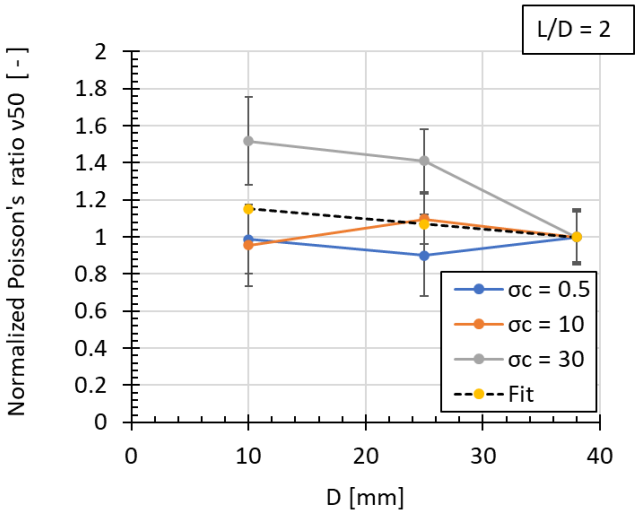

Fig. 18. Average normalized ν50 of all rocks vs. diameter for confining stress σ_c = 0.5, 10, and 30 MPa. All samples have L/D ratio equal to 2 Standard deviation and approximation of the data with Eq. (7) are also reported.

6.3 Combined shape and size effect

In this study, the tangent Poisson's ratio appears independent of the specimen shape. Therefore, only the size effect formula Eq. (7) is necessary to obtain the ν_{50} value of a specimen with arbitrary shape or size.

7 Conclusions

In this work, an experimental campaign has been performed to evaluate the effect of specimen size and shape on the mechanical properties measured on the small plugs that can be subsampled from field RSWCs. Indeed, few evidence are available in the literature on small specimens [9] of typical reservoir lithologies [1, 9].

Unlike the literature on larger specimens [1,2,3,4,5], rock strength for 10 mm diameter plugs decreases for decreasing L/D ratios, especially for L/D = 1 where, reasonably, damage during specimen coring and polishing can affect rock behaviour. The dependency of strength on size, instead, is coherent with evidence available in literature for diameters lower than 38-54 mm, where strength increases with size.

Stiffness, instead, is not influenced by the size of the specimen while increases with increasing L/D ratio due to the bedding effect. This problem may be eliminated if strain gauges or other local axial deformation measurements are used for plugs with low L/D ratio.

Dilation is not significantly affected by the shape of the specimen while it slightly decreases for increasing size.

The results of the tests were also quantitatively integrated to propose analytical equations that correlate strength, stiffness and dilation with both size and shape. These correlations will be useful in practical application to correlate the mechanical properties measured on small specimen retrieved from RSWCs with those that would have been measured through conventional plugs.

Previous observations suggest that small diameter specimens can be a useful tool for practical experimental rock characterizations involving RSWCs, but the use of only plugs

with L/D greater than 1.5, for which the effects of experimental artifacts is negligible, is recommended.
This study, based on experiments on dry plugs, was focused on the effects on the mechanical properties measurements of specimen geometry exclusively. Therefore, no saturation dependency was included in the proposed correlations. Anyway, future studies on saturated specimens with different shape and size could be desirable to understand the potential effect of the different allowed drainage paths during the experiments, especially for low permeability rocks.

Appendix. Method for correcting the inherent specimen variability though density measurements.

With the final aim of removing, as much as possible, the inherent specimen variability from the strength, stiffness, and dilation measurements, a procedure has been defined to quantify this variability based on dry bulk density measurements. A series of experiments were performed on three specimens for each lithology that were prepared from blocks characterized by different density to measure the variability of mechanical properties related to density variations. Burlington limestone was not tested since all block showed similar densities. All tests were run on specimens with L/D = 2, D = 38 mm, and at confining stress σ_c = 0.5 MPa. Figure 19 plots peak axial stress, stiffness modulus and Poisson's ratio as functions of dry density together with the linear regression of the data. Due to the limited number of data for each series, the linear approximation has been considered the most suitable: the deviation with respect to measured data is anyway small within the investigated density range, only Poisson's ratio shows higher dispersion.
The slopes a_σ, a_E and a_N of the linear approximations for the peak axial stress, the stiffness modulus and the Poisson's ratio respectively were used to define the following relations between the measured mechanical properties and the mechanical properties corresponding to a reference value of density:

$$\sigma_{ref} = \sigma_m + a_\sigma(\rho_{ref} - \rho_m)$$

$$E_{50ref} = E_{50m} + a_E(\rho_{ref} - \rho_m) \quad (8)$$

$$\nu_{50ref} = \nu_{50m} + a_N(\rho_{ref} - \rho_m)$$

where σ_m, E_{50m}, and ν_{50m} are, respectively, the peak axial stress, the stiffness modulus and the Poisson's ratio of a specimen with density ρ_m, while σ_{ref}, E_{50ref}, and ν_{50ref} are the corresponding values for the reference density. This reference density ρ_{ref} was assumed equal to the average density of all the specimens of a given lithology. The corrected mechanical properties σ_{ref}, E_{50ref}, and ν_{50ref} were then used in the analysis of experimental results to directly compare values corresponding to the same density.

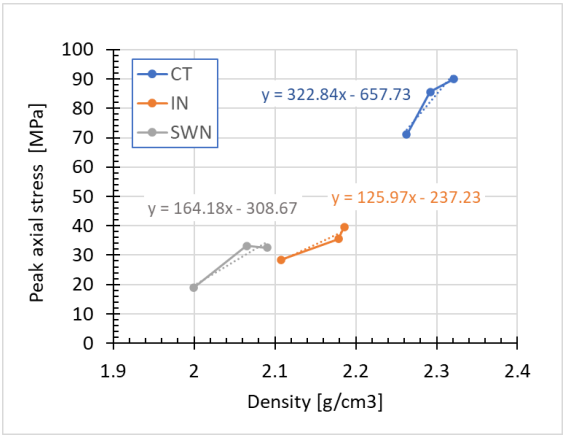

(a)

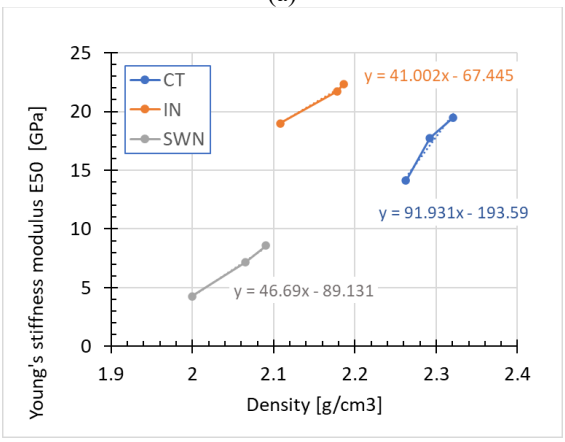

(b)

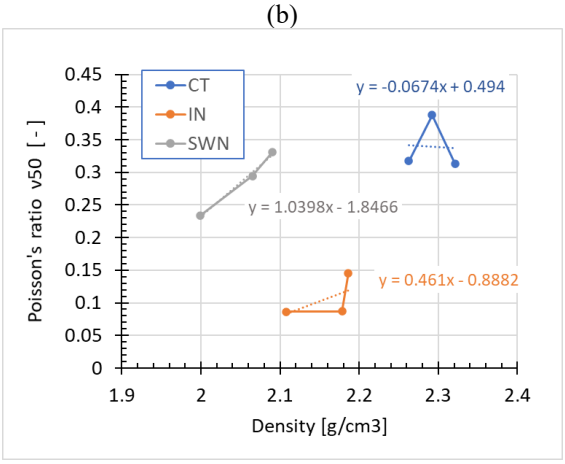

(c)

Fig. 19. (a) Peak axial stress, (b) Stiffness modulus E_{50}, and (c) Poisson's ratio ν_{50} vs. density for Carbon Tan (CT), Indiana (IN) and Saltwash North (SWN). The linear approximations to the data are also plotted.

References

1. U. Prasad, C. Wolfe, Formation specific size correction for strength (UCS) on rotary sidewall cores. *51st US Rock Mechanics/Geomechanics Symposium*, San Francisco, CA, ARMA17-534 (2017).

2. K. Mogi, Some precise measurements of fracture strength of rocks under uniform compressive stress. *Rock Mech. Eng. Geol.* IV, 41-55, (1966).

3. L. Obert, W.I. Duvall. Rock mechanics and the design of structures in rock. New York, Wiley, (1967).

4. L.A.A. da Silva, E.C. Sansone, J. Fujii, Shape effects considerations on the uniaxial compressive strength of hard rocks. *ISRM International Symposium EUROCK 93,* 1993-092, Lisbon, Portugal, (1993).

5. D.W. Hobbs, Rock compressive strength. Colliery Engineering 41, 287-292, (1964).

6. ASTM, Standard test method of unconfined compressive strength of intact rock core specimens. D 2938: 390–391, (1986).

7. K. Mogi, The influence of the dimensions of specimens on the fracture strength of rocks – Comparison between the strength of rock specimens and that of the Earth's crust. *Bulletin of the Earthquake Research Institute,* 40, 175-185, (1962).

8. E. Hoek, E.T. Brown, Underground excavations in rock. *The Institution of Mining and Metallurgy*, London, Chapman & Hall, (1980).

9. A. B. Hawkins, Aspects of rock strength. *Bulletin of Engineering Geology and the Environment* 57, 17–30, (1998).

10. P. Dirige, J. F. Archibald, The effects of geometry on the uniaxial compressive strength properties of intact rock core specimens. *Golden Rocks 2006, 41st US Symposium on Rock Mechanics*, Golden, CO, ARMA/USRMS 06-1016 (2006).

11. K. Thuro, R.J. Plinningr, S. Zah, Scale effect in rock strength properties, *Eurock 2001: Rock Mechanics a challenge for society*. Espoo, Finland, 169-174, (2001).

12. D. A. Moronkeji, U. Prasad, J. A. Franquet, Size effects on triaxial testing from sidewall cores for petroleum geomechanics. *48th US Rock Mechanics /Geomechanics Symposium.*, Minneapolis, MN, ARMA14-7405, (2014).

13. F. Nunes, V. Cavaleiro, L. Oliveira e Sousa, Scale effect of granitic materials. *45th US Rock Mechanics/Geomechanics Symposium.*, San Francisco, CA, ARMA 11-373, (2011).

14. E. Papamichos, J. Tronvoll, I. Vardoulakis, J. F. Labuz, A. Skjærstein, T. E. Unander, J. Sulem, Constitutive testing of Red Wildmoor sandstone. *Mechanics of Cohesive-Frictional Materials* 5, 1, 1-40, (2000).

15. A.H.J. Al-Rkaby, Z. M. S. Alafandi. Size effect on the unconfined compressive strength and modulus of elasticity of limestone rock. *Electronic Journal of Geotechnical Engineering* 20, 12, 5143-5149 (2015).

16. A.S. Abou-Sayed, C. E. Brechtel, Experimental investigation of the effects of size on the uniaxial compressive strength of Cedar City quartz diorite. *17th Symposium on Rock Mechanics*, Snowbird, UT, Paper 5 D6, (1976).

17. H. Masoumi, K. J. Douglas, S. Saydam, P. Hagan, Experimental study of size effects of rock on UCS and point load tests. *46th US Rock Mechanics / Geomechanics Symposium.*, Chicago, IL, ARMA 12-215 (2012).